IJBCS ISSN: 2147-1428

Orginal Article

International Journal of Basic and Clinical Studies (IJBCS)

2020; 9(2): 76-87 Yildiz ZA. Et all.

Multiparametric Evaluation of Soft Tissue Lesions by Shear Wave Elastography, Diffusion Weighted Imaging and Perfusion MRI

Yunus Emre Akpinar[1] Zuhal Bayramoglu[2] Ravza Yilmaz[2] Ahmet Salduz[3] Memduh Dursun[2]

[1] Biruni University Hospital Department of Radiology Istanbul, 34010 Turkey
[2] Istanbul University, Medical Faculy Department of Radiology Istanbul, 34010 Turkey
[3] Istanbul University, Medical Faculy Department of Ortopedi and Traumatology Istanbul, 34010 Turkey

Abstract

We aimed to investigate diagnostic accuracy of shear wave elastography (SWE), diffusion weighted imaging (DWI) and perfusion magnetic resonance imaging (p-MRI) in differentiation of benign and malignant soft tissue masses.

SWE, DWI and p-MRI were performed in 23 histopathologically proven (13 benign and 10 malignant) soft tissue lesions (15 female, 8 male; mean age: 46.43 ± 15.79 years).Quantitative evaluation of the masses with SWE in kilopascals, quantitative apparent diffusion coefficient (ADC) measurements of the lesions on DWI were performed.The perfusion curves of the lesions were also drawn on dynamic contrast enhanced MRI images.

Malignant lesions were significantly larger compared to the benign lesions (p= 0.008). No significant difference was found among mean elasticity values (p>0.05) and mean ADC values of benign and malignant lesion groups (p=0.059), but ADC values in the malignant group were in trend to be lower than benign lesions.When a cut-off value for differentiation of benign and malignant lesions was set to 1.06 10^{-3} mm^2/second; the sensitivity, specificity, positive and negative predictive values along with diagnostic accuracy for detection of malignant lesions was found to be 87.5%, 58.3%, 58.3%, 87.5%, 75%, respectively.Type 4 perfusion curve was more commonly seen in malignant lesions (57.1% of malignant lesions (p = 0.045) compared to benign lesions and type 2 curve was commonly encountered in benign lesions (54.5% of benign lesions).

Soft tissue tumors constitute a heterogeneous group with a broad range of elasticity characteristics. In contrast to diffusion and perfusion MRI, the diagnostic accuracy of SWE is not sufficient to differentiate malignant from benign soft tissue tumors in isolation. We demonstrated that p-MRI would provide more accurate results compared to elastography and diffusion weighted MRI examination. Diffusion and perfusion weighted studies would be added to conventional MRI sequences.

Key words: Soft tissue tumors, Shear wave elastography, Diffusion weighted imaging, Perfusion weighted imaging

IJBCS ISSN: 2147-1428

Orginal Article

International Journal of Basic and Clinical Studies (IJBCS)

2020; 9(2): 76-87 Yildiz ZA. Et all.

Introduction

Soft tissues develop from mesodermal origin including fibrous connective tissue, adipose tissue, skeletal muscle, blood/lymph vessels and peripheral nervous system that support specific tissues. In general, the incidence of benign soft tissue tumors is approximately 10 times higher than that of malignant soft tissue tumors (1).Parameters in evaluation of soft tissue tumors could be given as location, growth pattern, probability of recurrence, distribution and presence of metastases, patient's age to be aware of prognosis. The treatment plan for the soft tissue tumors requires multidisciplinary approach to reduce local recurrence. Since consecutive resections are also difficult to perform and surgical margins are important in decision making for adjuvant therapies; to detect the lesion, determine lesion composition, predict the tissue that the tumor originated, rule out the malignancy and determine invaded surrounding structures by preoperative imaging findings are crucial.

Soft tissue tumors constitute a heterogeneous group. Malignant lesions are expected to present with higher cellularity, lower doubling time, and necrosis. Consequently, malignant lesions are expected to show lower ADC values due to cellularity and demonstrate different enhancement patterns, when compared to benign lesions.

Materials and Methods

Patient Selection and Research Protocol

Our study was carried out between April 2017 and December 2017 by enrolling 23 patients (15 females, 8 males) aged between 15-70 years and who had been referred to radiology department from the orthopaedic clinic of the hospital with the initial diagnosis of a soft tissue tumor. Initial ultrasonographic examination was performed by a radiologist having 5 years of ultrasound and MRI experience. The lesions that previously underwent incisional or core needle biopsy were excluded. The patients underwent SWE examination followed by multiparametric MRI evaluation regarding DWI and p-MRI. This study was approved by local ethics committee (File number: 2017/1195). Because novel ultrasound applications as SWE and dynamic contrast enhanced sequences with diffusion weighted images on MRI have been routinely performed for further evaluation of the tumors in our department and since the data were collected retrospectively, we did not achieve the patients for informed consents.

We used an ultrasound device equipped with SWE application (Canon, Aplio 500 Platinium (Japan)). A lineer probe with 12 and 14 MHz frequency was used for the lesions that are 0.5 cm to 7.3 cm in depth. A total of 22 lesions were enrolled in SWE evaluation. Only one patient underwent MRI without SWE examination.

A chromatic scale was set to 0-150 kPa on SWE. The hardest area corresponded to dark red in the chromatic spectrum from red to blue with. A gel pad with a thickness of at least 0.5 cm

was used for the examination of the superficial lesions that were less than 1 cm in depth. Necrosis and internal hyperdynamic flow were also depicted. Quantitative measurements were obtained from solid and non-necrotic areas marked as the hardest area on chromatic scale. The patient was warned to be stationary during examination. Since cystic necrotic and calcific parts and deep lesion parts around the bones cause artifacts, these areas were avoided to obtain SWE examinations.The measurements were obtained within a depth ranging 1 to 7 cm. The probe was placed perpendicularly to the skin and also short axis of the lesion. At least three regions of interest (ROIs) that were 2-4 mm in diameter were selected and median stiffness values in kPa for each lesion were determined for statistical purposes.

The patients underwent both DWI and p-MRI (Achieva 3.0 TX– series, Philips Medical System 2013, 3 Tesla magnetic field strength) within the same week with the SWE examination prior to the histopathological examinations. Routine anatomical imaging was performed by obtaining T1-weighted and T2-weighted sequences followed by DWI and p-MRI consecutively. MRI sequence parameters were adjusted according to the size of the lesions and the size of the examination area which are indicated in the Table 1.

Table 1: Parameters of diffusion and perfusion sequences on magnetic resonance imaging "TR: Time of repetition, TE: Time of echo"

Time of acquisition:	3:25	**Time of acquisition:**	6:00
Field of view (FOV):	20-30 cm	**Field of view (FOV):**	280 cm
TR :	3164 ms	**TR :**	3.5 ms
Matrix size:	76x84	**Matrix size:**	140x187
TE:	72 ms	**TE:**	1.64 ms
EPI factor:	69	**Flip angle**	22 degrees
b value:	0 – 1000 s/mm	**Section thickness:**	3-7 mm
Number of signal average:	3	**Cross section:**	2-5 mm
Section thickness:	5 mm	**Number of signal average:**	2

Quantitative DWI and p-MRI evaluations were processed at the workstation (Philips Extended Mr Work Space 2.6.3.5 (Philips Medical Systems Nederlands BV 2013) workstation) by a radiologist experienced in musculoskeletal radiology at least 5 years. DWI-MRI was performed in a total of 20 lesions (malignant:8 benign:12). Three patients who underwent MRI with a different device were not included in MRI evaluations but included for SWE examinations. In addition, two of the participants had renal dysfunction, therefore perfusion MRI with contrast administration could not be performed, only DWI MRI data were recruited. A total of 18 patients with available p-MRI data were investigated. The MultiTransmit Single

Shot SE –EPI sequence was used for DWI.Two different b values (b = 0 and b = 1000 s / mm2) were used to generate an ADC map. Quantitative diffusion data were obtained on ADC maps. Once equivalent of the brightest area of DWI was detected, than quantitative ADC measurements were obtained by drawing ROIs as large as possible by free hand technique on ADC map. At least three different ADC values were obtained for each lesion and median ADC values were selected for statistical purposes.

T1-weighted Turbo Field Echo sequence was obtained for p-MRI. During this examination, a single dose of 0.2 mmol / kg Meglumine Gadoterate (Dotarem) bolus was administered intravenously and the maximum dose was limited to 20 ml. Injection rate was determined as 2.5 ml / sec by an automatic pump. The perfusion curves were generated from the lesion parts that represent intense contrast enhancement in the early phase. The parts were marked on the lesion and the perfusion parameters along with the curve type were generated automatically by the device.

The quantitative radiological data were compared among benign and malignant lesions. Eighteen of the cases had histopathological evaluation and the remaining five mass were finally diagnosed as (e.g. lipomas, hemangiomas) based on specific imaging characteristics and medical history of the patient.

Statistical Analysis

NCSS (Number Cruncher Statistical System) 2007 (Kaysville, Utah, USA) program was used for the statistical analysis. Descriptive statistics regarding mean, standard deviation, median, frequency, rate, minimum, maximum along with Mann-Whitney U test for the two group comparisons with non-normal distribution were used. Fisher-Freeman-Halton test and Fisher's Exact test were used to compare the qualitative data. The level of significance was accepted as $p<0.05$.

Results

Mean age of the participants was 46.43±15.79 years. Thirteen (n:13; 56.5%) of the lesions were benign and the remaining were malignant (n = 10; 43.5 %). The histopathological diagnosis of the cases were given in Table 2. The masses were commonly located at the lower extremities (n:14; 60.9%) and the remaining were located at the upper extremities (n:9; 39.1%) (Table 2).

IJBCS ISSN: 2147-1428

Orginal Article

International Journal of Basic and Clinical Studies (IJBCS)

2020; 9(2): 76-87 Yildiz ZA. Et all.

Table 2: Lesion Characteristics

Lesion Characteristics				
Pathology result		**Benign lesion: n:** 13**;** 56.5 **%** **Malign lesion: n:** 10; 43.5%		
Localisation		**Lower extremity: n:** 14; 60.9 % **Upper extremity: n:** 9; 39.1 %		1.0 [b]
DWI	**Lesions (n)**	**ADC**		0.059[a]
		Median	**Range**	
	Total: 20 **Benign (12):** **Malignant (8):**	**1** **1.2** **0.8**	0.1-2.2 0.5-2,2 **0.1-2**	
Perfusion MRI; **N: 18**	**Type 2 (B-M)** **Type 3 (B-M)** **Type 4 (B-M)** **Type 5 (B-M)**	**n:** 8 (6-2) **n:**4 (3-1) **n:** 4 (0-4) **n:**2 (2-0)	(44.4) (22.2) (22.2) (11.2)	0.045[c]
SWE	**Lesions (n)**	**Elasticity (kPa)**		0.385[a]
		Median	**Range**	
	Total : 22 **Benign (13):** **Malignant(9)**:	84.5 45.8 98	8.7-144 8.7-144 14-144	

[a]Fisher's Exact [b]Mann Whitney U Test [c] Fisher Test Freeman Halton Test "Lesion Characteristics . "B: Benign, M: Malignant, DWI: Diffusion weighted imaging, ADC: Apperent Diffussion Coefficient, Std.Dev. : Standart Deviation, MRI: Magnetic Resonance Imaging, SWE: Shear Wave Elastography

The mean age of the patients with assessed benign masses was 44.46±14.58 years, while this was 49.00±17.69 years for malignant lesions. 69.2% (n = 9) of the benign cases and 60.0% (n = 6) of the malignant cases were females. There was no statistically significant difference among median ages and gender distribution of the patients with benign and malignant lesions (p> 0.05).

Benign lesions were located at lower extremity in 61.5% (n = 8) and upper extremity in 38.5% (n = 5) of the participants. Malign lesions were located at lower extremity in 60.0% (n = 6) and the remaining were located at the upper extremity (40.0% (n = 4)). There was no statistically significant difference between benign and malignant lesions in terms of the localization (p> 0.05)(Table 2).

Mean shear wave elasticity was 78.45±47.57 kPa (range: 8.7–44.8 kPa, median: 84.5 kPa) in general, 69.49±50.71 kPa (median: 45.8 kPa) in benign and 91.40±42.02 kPa (median: 98 kPa) in malignant lesions. Differences of median SWE values were not statistically significant (p> 0.05) (Table 2).

Mean ADC values were 1.05±0.57 x 10^{-3} mm^2/second (median: $1x10^{-3}$ mm^2/second) in general, this was $0.79±0.61x10^{-3}$ mm^2/second (median: $0.8x10^{-3}$ mm^2/second) in the malignant group, and $1.23±0.50x10^{-3}$ mm^2/second (median: $1.2x10^{-3}$ mm^2/second) in the benign group. There was no statistically significant difference among ADC values of benign and malignant lesions (p:0.059). However, ADC values were in trend to be lower in malignant lesion group. Receiver operating characteristic curve (ROC) analysis and diagnostic screening tests were used to determine a cut-off point for predicting malignancy. When the cut-off point for ADC was set to $1.06x10^{-3}$ mm^2/second; sensitivity, specificity, positive predictive value and negative predictive value were 87.50%, 58.33%, 58.33% and 87.50%, respectively (Table 3). Area under the curve was found to be 75% with a

IJBCS ISSN: 2147-1428

Orginal Article

International Journal of Basic and Clinical Studies (IJBCS)

2020; 9(2): 76-87 Yildiz ZA. Et all.

standard error of 1.2% in the ROC curve (Fig. 1). The Odds ratio of ADC (lower than 1.06x10-3 mm2/sec) for suggesting malignancy was 9,800 (95% CI: 0.899-106.845).

Table 3: Diagnostic Screening Tests, ROC Curve and Pearson Chi-Square Test* Results for ADC . "PPV: Positive Predictive Value, NPV: Negative Predictive Value, AUC: Area Under Curve"

	ROC Curve	**Cut-off**	**Sensitivity (%)**	**Specificity (%)**	**PPV (%)**	**NPV (%)**	**AUC (%)**	**p**
ADC value		<1.06	87.5	58.3	58.3	87.5	75	0.032
				Benign Lesion		**Malign Lesion**		**p**
				n	**Frequency (%)**	n	**Frequency (%)**	
	Pearson Chi-Square Test		<1.06	5	41.7	7	87.5	0.04*
			>1.06	7	58.3	1	12.5	

When perfusion curve types were examined; 54.5% (n = 6) of the benign lesions represented type 2, 27.3% (n = 3) represented type 3 and 18.2% (n = 2) represented type 5 curves. No benign case was found to be compatible with type 1 and type 4 enhancement curve. Among malignant lesions, perfusion curve types were type 2 in 28.6% (n = 2), type 3 in14.3% (n = 1) and type 4 in 57.1% (n = 4).

No type 1 and type 5 curves were observed among malignant lesions. There was a statistically significant difference between perfusion curve types among benign and malignant lesions (p = 0.045);

type 4 curve was found to be significantly higher in malignant lesions compared to the benign lesions.

The raw datas obtained are presented in table 4.

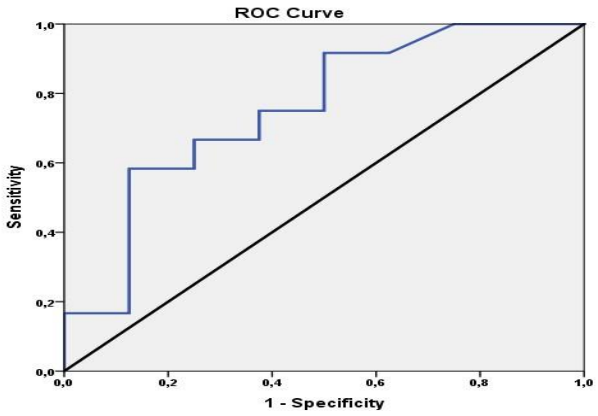

Figure 1: ROC curve for quantitative ADC values for detection of malignancy.

IJBCS ISSN: 2147-1428

Orginal Article

International Journal of Basic and Clinical Studies (IJBCS)

2020; 9(2): 76-87 Yildiz ZA. Et all.

Table 4 : Histopathologic diagnosis and obtained datas of cases

Gender	Patient	Age	Location	Histopathologic Diagnosis	Nature	ADC Value (10^{-3} m^2/s)	Perfusion Curve Type	Size (mm)	SWE (kPa) (Maximum)
FEMALE	1	40	UE	GIANT CELL TENDON SHEATH TUMOR	B	1.212	5	9x15x7	117
FEMALE	2	31	LE	FIBROGRANULOMA	B	0.512	2	11x17x13	139.2
MALE	3	55	LE	HIGH GRADE FUSIFFORM CELL SARCOMA (GRADE 3) RABDOMIOSARCOMA	M	0.520	2	194x114x131	130.4
MALE	4	53	LE	PIGMENTED VILLONODULAR SYNOVITIS-TENOSINOVAL GIANT CELL TUMOR	B	0.816	2	45x25x37	21.8
FEMALE	5	15	UE	ROUND CELL MALIGN TUMOR (EXTRAOSSEOUS EWING)	M	0.113	-	29x31x26	78.9
FEMALE	6	45	LE	BIPHASIC TYPE SYNOVAL SARCOMA	M	0.894	4	67x57x45	98.8
MALE	7	70	UE	NEUROFIBROMA	B	1.147	3	52x21x23	144
FEMALE	8	50	LE	SPINDLE CELL PROLIFERATION WITH SMOOTH MUSCLE PHENOTYPE	B	1.034	2	53x39x48	117.2
MALE	9	30	UE	SPINDLE CELL MYOFIBROBLASTIC TUMOR	B	1.385	3	22x14x11	125.5
FEMALE	10	34	LE	HEMANGIOMA	B	1.360	-	35x15x11	23.2
FEMALE	11	61	LE	TENOSYNOVIAL GIANT CELL TUMORS	B	0.969	3	71x78x28	45.8
FEMALE	12	63	UE	WELL-DIFFERENTIATED LIPOSARCOMA	M	-	-	113x126x65	14
MALE	13	63	LE	FUSIFORM CELL SARCOMA	M	1.063	4	52x191x51	90
FEMALE	14	56	UE	SPINDLE CELL MESENCHIMAL TUMOR (LOW GRADE SUB-TYPE NON-DETERMINABLE SARCOMA)	M	0.139	2	23x18x19	42.5
FEMALE	15	45	LE	FIBROGRANULOMA	B	2.043	5	59x20x22	53.4
FEMALE	16	59	LE	MALIGNANT MELANOMA	M	0.611	4	37x35x10	98
FEMALE	17	56	LE	LYMPHANGIOMA	B	2.245	2	18x24x10	44
FEMALE	18	17	LE	HEMANGIOMA	B	1.303	2	22x19x50	18.6
MALE	19	53	UE	ANGIOLIPOMA	B	0.846	2	20x20x10	45
FEMALE	20	61	UE	CHONDROSARCOMA	M	2.276	4	60x46x40	126
FEMALE	21	38	UE	LIPOMA	B	-	-	24x8x52	8.7
MALE	22	54	LE	SYNOVIAL SARCOMA	M	1.065	3	108x67x91	-
MALE	23	19	LE	SOFT TISSUE RECURRENT OSTEOSARCOMA	M	-	-	49x33x24	144

.B: Benign, M: Malignant, UE: Upper Extremity, LE: Lower Extremity

IJBCS ISSN: 2147-1428

Orginal Article

International Journal of Basic and Clinical Studies (IJBCS)

2020; 9(2): 76-87 Yildiz ZA. Et all.

Discussion

Soft tissue tumors constitute a very heterogeneous group of tumors that originate from a wide variety of tissues with many histopathological subtypes. Being aware of the extent of the lesion, surrounding functional structures (neurovascular bundle, fascia) and to depict invasive behaviour have been crucial in the management of the patient and predict prognosis. In this study, the quantitative data were obtained with different imaging modalities by using novel applications to reveal whether tissue stiffness by SWE, diffusion properties by DWI- MRI and perfusion kinetics by p-MRI would be able to differentiate malignant from benign lesions.

Diffusion of water molecules in biological tissues depends on the ratio of intracellular and extracellular spaces in the tissues. Decreased cellularity would increase diffusibility by relatively increased ratio of the extracellular space (2). High cellularity observed in malignant soft tissue sarcomas, results in diffusion limitation and reduced quantitative ADC values. Intact cell membranes, tight connections between the membranes, fibers, macromolecules and cellular organelles will cause lower ADC values by limiting the movement of water molecules. Tumor lysis as a result of cytotoxic treatment would cause disorganization of the membrane integrity and inter-membranous associations resulting in increased ratio of extracellular space and the efficacy of the treatment could be evaluated using a non-contrast imaging study such as DWI (3). In this study, we investigated the differentiation of benign and malignant soft tissue masses by quantitative ADC measurement. It is simple and reproducible to use an observer-based ROI placement method in the area of the lowest visual signal within the image. Many authors tend to report average ADC values as we assessed in this present study. We suggest to evaluate masses with DWI because of the tendency to reveal lower ADC values than $1.06x10^{-3}$ mm^2/second. However, we found ADC values of angiolipoma, fibrogranuloma, spindle cell proliferation, giant cell tendon sheath tumor $<1.06x10^{-3}$ mm^2/second with fibrogranuloma presenting lowest ADC values among theese benign lesions. Giant cell tendon sheat tumors include various amounts of mononuclear histiocytic cells, multinuclear giant cells, collagen and, xanthoma cells frequently containing hemosiderin granules (4). Additionally, since these tumors contain no necrotic-cystic or myxoid degeneration areas, the quantitative ADC values expected to be quite low. Maeda et al. found no significant difference among ADC values between benign ($1.50±0.64×10^{-3}$ mm^2/second) and malignant ($1.45±0.59×10^{-3}$ mm^2/second) soft tissue tumors (n: 44) (5). Einarsdóttir et al. examined a case series of 16 benign soft tissue lesions and 13 soft tissue sarcomas (6) and depicted closest mean ADC values as $1.8x10^{-3}$ mm^2/second in benign lesions, $1.7x10^{-3}$ mm^2/second in malignant lesions. Nagata et al. divided the subgroups as myxoid and non-myxoid tumors in 88 histopathologically verified cases (44 benign, 8 intermediate, 36 malignant) (7) and found significantly higher mean ADC values of myxoid tumors ($2.08±0.51x10^{-3}$ mm^2/second) compared to that of non-myxoid tumors ($1.13±0.40x10^{-3}$ mm^2/second) ($p<0.001$). However, no significant ADC difference was found between benign ($2.10±0.50x10^{-3}$ mm^2/second) and malignant ($2.05±0.58x10^{-3}$ mm^2/second) myxoid tumors while benign non-myxoid tumors ($1.31±0.46 x 10^{-3}$ mm^2/second) presented significantly higher ADC values compared to malignant non-myxoid tumors ($0.94±0.25 x 10^{-3}$ mm^2/second). Razek et al. retrospectively screened 37 patients with soft tissue masses (8) and depicted a cut-off value for ADC as $1.34x10^{-3}$ mm^2/second, distinguishing malignant nature of the lesions when ADC value was lower than this cut-off with 94% sensitivity and 88% specificity even differentiating high grade from low grade malignant soft tissue tumors. Although we had smaller sample size we obtained considerable diagnostic accuracy with an area under the ROC curve as 75 %.

In our study, chondrosarcoma was the tumor with the highest ADC value ($2.276x10^{-3}$ mm^2/second) among all benign and malignant lesions, although being malignant. Lowest ADC value ($0.113x10^{-3}$ mm^2/second) was found in extra-osseous ewing sarcoma among malignant and in post-op fibrogranuloma ($0.512x10^{-3}$ mm^2/second) among benign lesions. The overlap of the ADC values of benign and malign lesions and the factors causing these results should be investigated with larger scale studies including different types and grades of lesions.

There are several studies evaluating both normal stiffness ranges of tissues and also changes in case of inflammation, fibrosis and also malignant infiltration. Malignant lesions in especially breast and thyroid tissue have been distinguished by elastography with a considerable diagnostic confidence. We evaluated the lesions with SWE by quantitative assessment. We depicted relatively lower stiffness (69.49±50.71 kPa, median: 45.8 kPa) values in the benign group compared to malignant lesions (91.40±42.02 kPa, median: 98 kPa). However, there has been a significant overlap between elasticity values which may be caused the smaller number of cases in each category and heterogeneous tumor types. Different histopathological properties necrotic-cystic degeneration,

International Journal of Basic and Clinical Studies (IJBCS)

2020; 9(2): 76-87 Yildiz ZA. Et all.

calcific deposits and occasional accompanying inflammatory changes can be found in both benign and malignant soft tissue lesions and they greatly reduce the sensitivity of SWE. There have been several sonoelastography studies used in decision making either based on scoring systems on qualitative chromatic images or quantitative measurements as stiffness (kPa) or shear wave speed (m/sn) in evaluation of musculoskeletal system, connective tissue and lesions with neurovascular origin. Pass et al. performed SWE examination in 66 benign and 39 malignant soft tissue tumors revealing no difference by quantitative measurement (9). In contrary to this, in another recent study, Pass et al. have concluded that longitudinal shear wave velocity measurements obtained in the lesions were 30% lower in malignant lesions compared to benign lesions (15 malignant, 35 benign) along with a moderate correlation between transverse and longitudinal shear wave measurements (10). Another quantitative evaluation was performed by Tavare et al. (11), including 206 adult participants (malign: %38, benign:62 %) by MRI and SWE for soft tissue masses. Transverse and longitunal velocity measurements for benign and probable benign lesions have showed good diagnostic accuracy (AUC = 0.87 [95% confidence interval {CI}: 0.79, 0.95]), while it provided no additional diagnostic contribution for malignant and possibly malignant lesions. By this way, patients with benign and probable benign lesions would be followed-up carefully without an invasive prosedure.

Semiquantitative evaluation of the masses has also been conducted. Magarelli et al. examined 20 malignant and 12 benign lesions by using 5 scale sonoelastographic chromatic scoring system with 4 and 5 corresponding malignant lesions. They reported that malignant lesions significantly demonstrated a blue color (hard tissue) coding and red color coding (softer tissue) was predominant in benign lesions (12). Bhatia KS et al. evaluated cervical non-nodal mass lesions in 49 patients. Four different grades were determined according to the degree of solidity of the lesions and neurogenic tumors-neuromas, (epi)dermoids and metastases were found to have a high degree of solidity, while lipomas, lymphatic-venous malformations, thyroglossal duct cysts and branchial cleft cysts were found to have low solidity (13). Both quantitative assessment and semiquantitative scoring systems have added several diagnostic contributions but further studies with larger scale are needed.

In the dynamic contrast enhanced pMRI the data obtained during the first contrast transition show useful information for tissue vascularization and tumor perfusion (14). Intense vascularization and high capillary permeability cause early and intense contrast enhancement. With pMRI we could obtain quantitative information through time signal intensity curves that are classified as five different patterns (15) (Fig. 2).

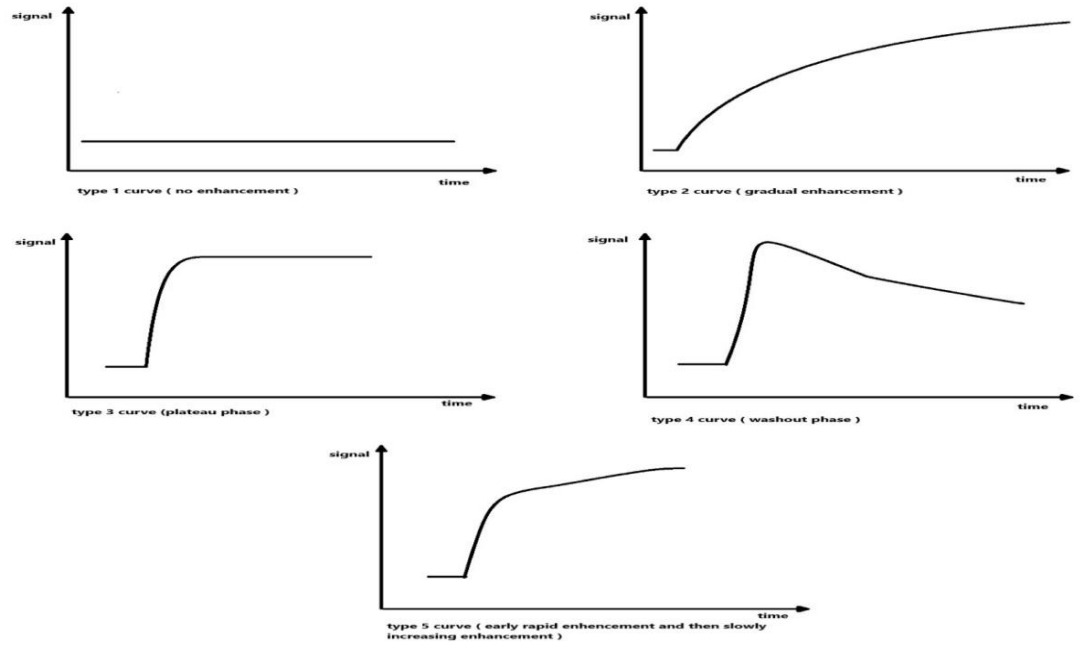

Figure 2: *Time - intensity curve types*

Type 1 is no enhancement by contrast material and can be seen especially in lipomas or hematomas . Type 2 is progressive increase in contrast enhancement observed especially in benign tumors. Type 3 corresponds subsequent plateau phase following rapid initial contrast enhancement phase which can be observed in a heterogeneous group such as vascularized benign tumors (desmoids tumors), abscesses and some malignant tumors that may not be useful in determining the nature of tumor tissue. Type 4 corresponds washout phase following rapid onset contrast enhancement which is seen in highly vascularised malignant lesions with a low interstitial space volume such as malignant fibrous histiocytoma, synovial sarcoma and leiomyosarcoma and benign tumors such as giant cell tumors. Type 5 shows slow enhancement in progressive form following rapid initial contrast enhancement that is seen in tumors after radiotherapy or chemotherapy or myxoid tumors with a large interstitial space.

In our study, a total of 18 cases had pMRI and 7 of them were in the malignant group. Among the malignant lesions, biphasic synovial sarcoma, malignant melanoma, fusiform cell sarcoma (Fig. 3a, 3b, 3c) and chondrosarcoma had type 4 time -intensity curve as expected, whereas spindle cell mesenchymal sarcoma with undifferentiated subtype and rhabdomyosarcoma (high grade) had type 2 and monophasic synovial sarcoma had type 3 time signal curves. Different subtypes of the main pathological diagnosis may represent also different time signal intensity curves. Barile et al. have created dynamic contrast-enhanced perfusion MRI-based signal time curves for 23 soft tissue tumors. In this study, two giant cell tumors and two myxofibrosarcomas were noted as the same histopathologically diagnosed tumors that represented different types of signal intensity curves.

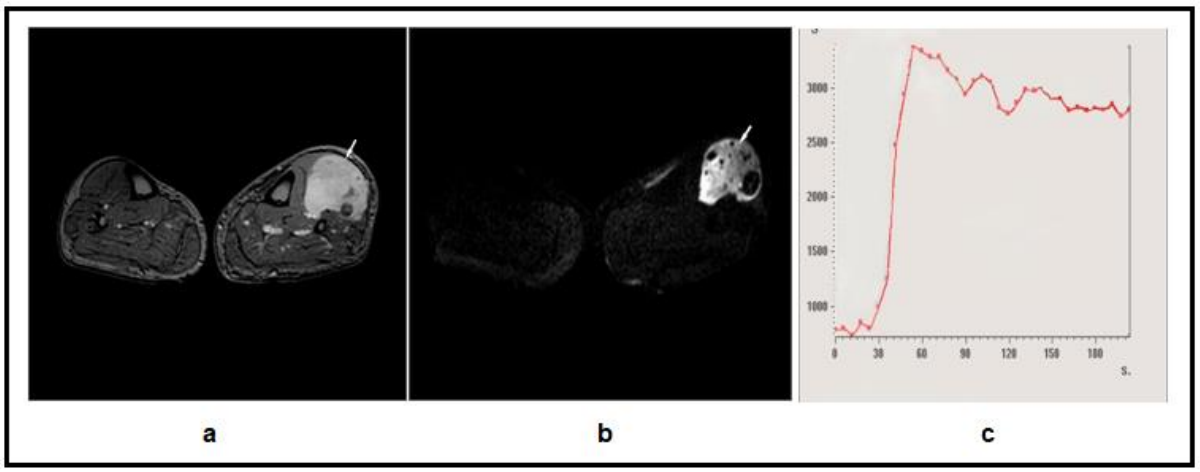

Figure 3: 63-year-old male patient with histopathologically confirmed fusiform cell sarcoma localized in the left crus is observed in (a)dynamic contrast-enhanced T1-weighted perfusion MRI on axial section image (arrow). (b) Significant diffusion restriction of the lesion is seen on axial section DWI image (b=1000). (c)Type 4 signal intensity time curve was obtained on perfusion MRI.

IJBCS ISSN: 2147-1428

Orginal Article

International Journal of Basic and Clinical Studies (IJBCS)

2020; 9(2): 76-87 Yildiz ZA. Et all.

Perfusion MRI data was classified quantitatively and maximum contrast and time to peak data were compared (16). Unlike our study, it was reported that type 4 curve type could be obtained in giant cell tumor but type 2 and type 3 curve patterns were obtained for this histopathologic type in our study (15, 16). Fibrogranuloma (Fig. 4a, 4b, 4c, 4d) (n: 2) and giant cell tumors (n: 2) in this study represented different types of enhancement curves both seen in benign and malignant lesions. The pMRI would reveal significant data about the viability of the lesions and this fact might be useful in investigating the efficacy of the treatment. The type 2 curve pattern seen in the high grade rhabdomyosarcoma case that had received radiotherapy in the preoperative period was notable since this type of curve is more frequently seen in benign lesions. the case was not excluded in order to measure the sensitivity of perfusion MRI study to evaluate tumor viability after treatment and compare with the literature.

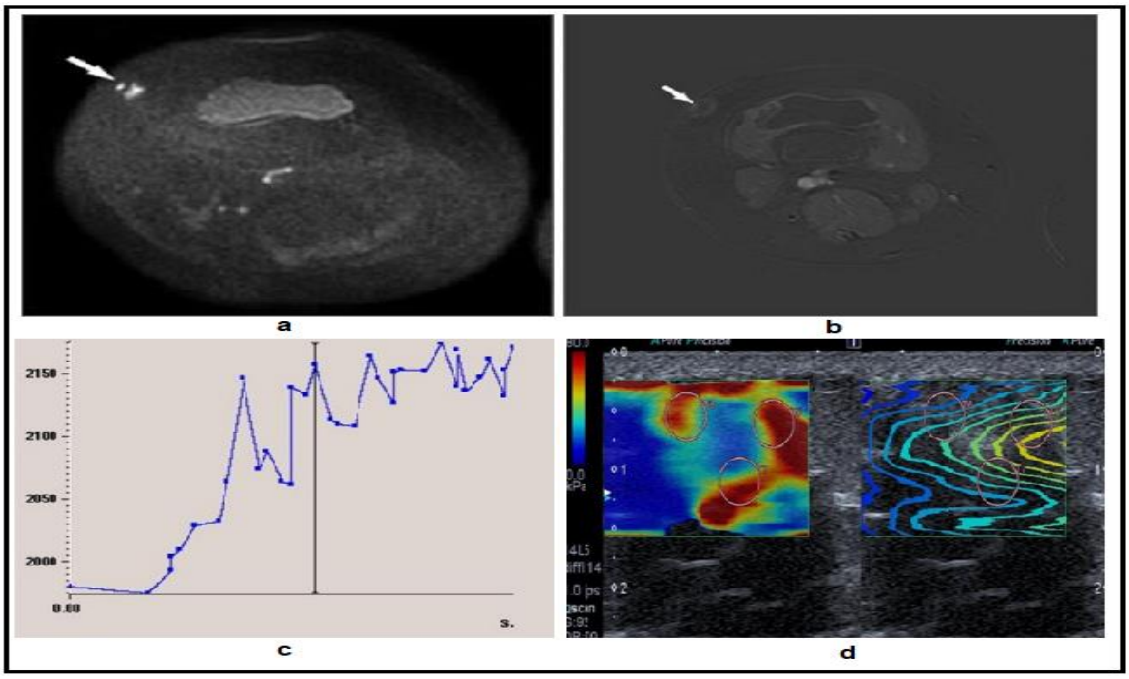

Figure 4: 31-year-old female patient. Mass lesion was depicted in subcutaneous fatty tissue in the anteromedial distal right thigh. The patient has a history of angiosarcoma excision. The lesion (arrow) is shown in axial section of DWI (a) and dynamic contrast-enhanced T1-weighted perfusion MRI with subtraction (b). Type 2 signal intensity time curve (c) supports the benign nature of the lesion. Chromatic scale of the lesion on SWE is seen (d). Histopathological diagnosis: Fibrogranuloma.

In the light of the data obtained, the majority of the malignant tumors had type 4 and type 3 curve patterns. Type 5 pattern which could be encountered in cases received radiotherapy and chemotherapy was not found in this present study. It was also significant that no type 4 curve pattern was observed in any of the benign tumors in our study ($p < 0.045$). p MRI would be superior than SWE and DWI in some cases, such as a palpable mass lesion at the operation site revealing a quite low ADC value and higher stiffness value by SWE suggesting recurrence. However, a type 2 curve by the p-MRI examination would conclude as a post-operative fibrotic reaction verified with histopathological evaluation. Although malignant tumors generally have a higher and faster contrast enhancement pattern compared to benign tumors, there may be occasional overlap between quantitative and qualitative data obtained in malignant tumors with poor vascularization and benign tumors with high vascularity (17). The all datas of the study are given in Table 4.

There are several limitations in this paper. First and the most important one is the limited number of patients evaluated by each modality. Due to the inability of the linear probe used in SWE to evaluate lesions in deep tissues,

superficially located limb masses were included in the study, therefore truncal lesions were excluded. Second, benign and malignant groups showed significant tumor heterogenity.

In conclusions; we demonstrated that p-MRI would provide more accurate results compared to elastography and diffusion weighted MRI examination. Diffusion and perfusion weighted studies would be added to conventional MRI sequences. The distinction between benign and malignant nature of soft tissue tumors among a heterogeneous histopathological spectrum may not always be easy. Therefore, correlation of clinical, radiological and pathological findings is usually necessary for accurate diagnosis and management of these lesions.

References

1. *Brys P. Magnetic Resonance İmaging: Basic Consepts. In: De Schepper AM, Vanhoenacker FM, Parizel PM, Gielen JL. Imaging of soft tissue tumors. Springer Science & Business Media, 2006; 71 - 83*
2. Schoeniger JS, Aiken N, Hsu E, Blackband SJ. Relaxation-time and diffusion NMR microscopy of single neurons. *J Magn Reson Imaging* 1994; Series B 103(3):261–273.
3. Moffat BA, Chenevert TL, Lawrence TS, et al. Functional diffusion map: a noninvasive MRI biomarker for early stratification of clinical brain tumor response. *Proc Natl Acad Sci U S A* 2005; 102(15):5524–5529.
4. Ahlawat S, Fayad LM. Diffusion weighted imaging demystified: the technique and potential clinical applications for soft tissue imaging. *Skeletal Radiol* 2018; 47(3):313–328.
5. Maeda M, Matsumine A, Kato H, et al. Soft-tissue tumors evaluated by line-scan diffusion-weighted imaging: Influence of myxoid matrix on the apparent diffusion coefficient. *J Magn Reson Imaging* 2007; 25(6):1199– 1204.
6. Einarsdóttir H, Karlsson M, Wejde J, Bauer HC. Diffusion-weighted MRI of soft tissue tumours. *Eur Radiol* 2004; 14(6):959–963.
7. Nagata S, Nishimura H, Uchida M, et al. Diffusion-weighted imaging of soft tissue tumors: usefulness of the apparent diffusion coefficient for differential diagnosis. *Radiat Med* 2008; 26(5):287–295.
8. Razek A, Nada N, Ghaniem M, Elkhamary S. Assessment of soft tissue tumours of the extremities with diffusion echoplanar MR imaging. *Radiol Med* 2012; 117(1):96–101.
9. Pass B, Jafari M, Rowbotham E, et al. Do quantitative and qualitative shear wave elastography have a role in evaluating musculoskeletal soft tissue masses? *Eur Radiol* 2017; 27(2):723–731.
10. Pass B, Johnson M, Hensor EM, et al. Sonoelastography of musculoskeletal soft tissue masses: a pilot study of quantitative evaluation. *J Ultrasound Med* 2016; 35(10):2209–2216.
11. Tavare AN, Alfuraih AM, Hensor EM, et al. Shear-Wave Elastography of Benign versus Malignant Musculoskeletal Soft-Tissue Masses: Comparison with Conventional US and MRI. *Radiology* 2019; 290(2):410–417.
12. Magarelli N, Carducci C, Bucalo C, et al. Sonoelastography for qualitative and quantitative evaluation of superficial soft tissue lesions: a feasibility study. *Eur Radiol* 2014; 24(3):566–573.
13. Bhatia KS, Rasalkar DD, Lee Y-P, et al. Real-time qualitative ultrasound elastography of miscellaneous non-nodal neck masses: applications and limitations. *Ultrasound Med Biol* 2010; 36(10):1644–1652.
14. van der Woude, H. J., Verstraete, K. L., Hogendoorn, P. C., Taminiau, A. H., Hermans, J., & Bloem, J. L. Musculoskeletal tumors: does fast dynamic contrast-enhanced subtraction MR imaging contribute to the characterization?. *Radiology*, 1998; 208(3): 821-828.
15. Drapé, J. L. Advances in magnetic resonance imaging of musculoskeletal tumours. *Orthopaedics & Traumatology: Surgery & Research*, 2013; *99*(1): 115-123
16. Barile A, Regis G, Masi R, et al. Musculoskeletal tumours: preliminary experience with perfusion MRI. Radiol Med 2007; 112(4): 550–561
17. Verstraete KL, Lang P. Bone and soft tissue tumors: the role of contrast agents for MR imaging. Eur J Radiol 2000; 34(3):229–246.